Full Length Research Paper

Tailoring wind properties by various passive roughness elements in a boundary-layer wind tunnel

Kapil Varshney

Research Department Manager, Taitem Engineering, PC Ithaca, NY 14850 USA.
110 South Albany Street, Ithaca, NY-14850, USA. E-mail: kvarshney@taitem.com. Tel: 413 658 7278.

Boundary-layer wind tunnel provides a unique platform to reproduce urban, suburban and rural atmospheric boundary layer (ABL) by using roughness devices such as vortex generators, floor roughness, barrier walls, and slots in the extended test-section floor in the contraction cone. Each passive device impacts wind properties in a certain way. In this study, influence of various passive devices on wind properties has been investigated. Experiments using eighteen different configurations of the passive devices have been carried out to simulate urban, sub-urban, and rural climate conditions in a boundary-layer wind tunnel. The effect of each configuration on the wind characteristics is presented. It was found that higher barrier height and more number of roughness elements on the floor, generated higher turbulence and therefore higher model scale factors were obtained. However, increased slot width in the extended test-section floor in the contraction cone of the wind tunnel seemed to have a little effect on wind characteristics.

Key words: Atmospheric boundary layer, wind tunnel, wind properties, roughness elements, turbulence.

INTRODUCTION

For a century, knowledge of simulation of atmospheric boundary layer (ABL) in the wind tunnel and deter-mination of correct model scale factor has continuously been growing. Accurate estimation of wind properties is essential in structural and physical design of big structures such as high-rise buildings, long-span bridges, tall towers, and chimneys. Wind tunnels have been used to determine aerodynamic characteristics of wind over different terrains for more than five decades. However, accurate boundary layer flows near the earth's surface are characterized by conditions which are generally not available to wind tunnels. In addition, non-uniform boundary conditions, variable atmospheric and thermal conditions encountered in practical situations make accurate prediction of the ABL flows extremely difficult.

The most common procedure to reproduce natural turbulent wind in a wind tunnel is by passing the wind through passive roughness devices which consists of roughness bars on the floor, barriers, spires etc. (Counihan, 1975; Tieleman et al., 1978; Reinhold et al., 1978; Farell and Iyengar, 1999; Kozmar, 2010; Kozmar 2011; Varshney and Poddar, 2011). Experiments are necessarily difficult although recent advances in techniques

have provided some improvements. In a recent work, artificial neural network (ANN) has been employed to determine wind properties (Varshney and Poddar, 2012). The ANN program was first trained by known experimental data and then it was used to predict wind properties for the other experimental data which were not used to train the model. The predicted wind properties fairly match with the experimental data.

Accurate and rapid responses from transducers are essential to determine various types of fluid properties (Cramer et al., 2006; Varshney and Panigrahi, 2005; Varshney et al., 2011a, b). In the cases when fluid is still and an object is freely-falling, high-speed cameras are being used to determine the 3-D orientation and the object speed (Varshney et al., 2012). Measurement of velocities is relatively simple however accurate calculations of turbulence level and then the integral length scales are important which are required for accurate prediction of wind-induced loads and aero-elasticity in structures. In general, simulating Reynolds number, $R_e = \overline{U} d / \nu$, which is based on mean velocity and the characteristic building dimension is important but
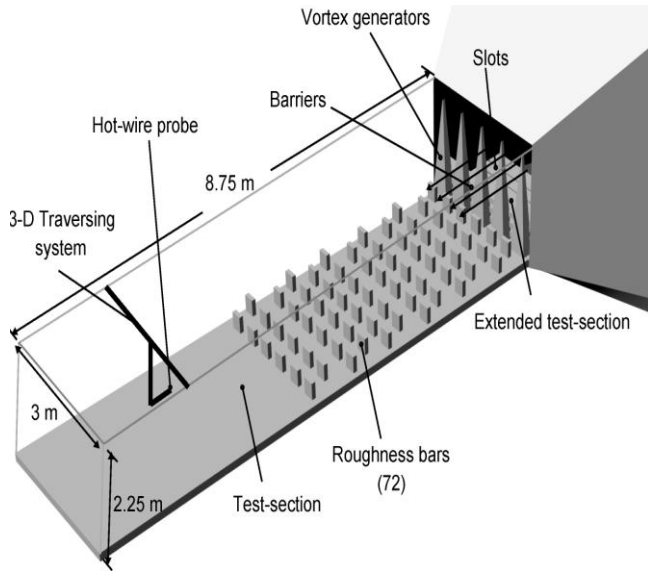
Figure 1. Arrangement of simulation-hardware in national wind tunnel facility (NWTF).

but due to geometric limitations, it becomes difficult to simulate 'R_e' in a wind tunnel. Further, in a wind tunnel, turbulent boundary layer develops over a smooth floor; however it requires a long test section to grow to an adequate thickness. In order to cope with this situation, the use of passive roughness devices becomes important.

The use of passive devices is very well documented. Counihan's (1969, 1971, 1973, 1975) method to use vortex generators, surface roughness, and castellated barrier to reproduce ABL, is widely accepted which has been adopted in this study. In his work, elliptical shaped wedge vorticity generators, combination of roughness elements, and barriers were used to simulate ABL. Counihan suggested that the boundary layer height is affected very little by changes in terrain roughness. Cook (1978a, b) further improved his methods by using other roughness devices such as castellated barriers, toothed barriers, wood blocks etc.

Many attempts have been made to duplicate a "typical" ABL in a wind tunnel. Due to time dependent variations in wind properties for a region, it becomes difficult to define the characteristics of ABL. ESDU data are commonly used as the prototype data (ESDU 1974-1975). Boundary layer height is a function of terrain type. Standard heights for rural and urban terrains were presented by Davenport and Isyumov (1967).

In this study, eighteen different configurations of passive devices such as two different sets of roughness elements on the floor, five "spires", three barrier walls, and slot width in the extended test section in the contraction cone, have been used to reproduce a wide range of rural to urban terrains. The effect of various passive devices on the wind characteristics is presented.

EXPERIMENTAL SET-UP AND MEASUREMENT PROCEDURE

Figure 1 shows the experimental set-up to simulate ABL. Measurements were conducted in a closed-circuit wind tunnel with a *8.75 m* long rectangular test-section of cross-section *2.25 x 3 m*. The wind tunnel was specially designed for aerodynamic applications. A single-wire hot-wire probe was used to acquire the time-dependent velocity signals. A single stage 12-bladed axial-flow fan regulated by a 1 MW variable speed DC motor was used to circulate the air in the wind tunnel from 3 to 80 m/s with a centerline turbulence level of <0.1%. A single-wire hot wire probe was used to measure velocity time-series at a sampling rate of 3000 Hz. The data were collected at *80* vertical positions in the center of the wind tunnel and *0.5 m* downstream from the last row of the roughness elements. Detailed description of the wind-tunnel, the arrangement of roughness elements, and experimental methodology are given in Varshney and Poddar (2011, 2012).

Atmospheric boundary layer simulation

A Wollaston wire of *5* micro meter in diameter, with a *1 mm* long sensing element, was operated in a constant temperature circuit at overheat ratio of 1.5 and used to measure velocities at *0.5 m* downstream from the last row of the roughness elements. The measurements were taken at 80 vertical locations for each configuration. A 3-D traversing unit was used to put the hot-wire probe at a desired location. To obtain shear velocity, the method proposed by Perry and Joubert (1963) was used. Mean velocity, turbulence intensity, power-law index, and shear velocity were calculated using the equations presented in Table 1. Determination of integral length scale requires auto-correlation coefficient and once the integral length scale factor is calculated, model length scale factor can be determined using the procedure proposed by Cook (1978a, 1978b). Autocorrelation coefficient, integral length scale, and model length scale factor can be calculated using the set of equations presented Table 2.

RESULTS AND DISCUSSION

Eighteen different configurations of the passive devices have been used in this study and the results are presented in Table 3 (Varshney and Poddar, 2011). Based on the procedure mentioned previously, wind characteristics for each configuration are determined. In these experiments, all five vortex generators were used in all configurations whereas the numbers of other passive devices such as roughness bars on the floor, barrier height, and slot width in the extended test section in the contraction cone have been varied. Typical wind properties using configuration 5 simulation hardware are shown in Figure 2.

Effect of barrier height on the wind characteristics

Change in the barrier height affects the wind characteristics significantly. The aerodynamic roughness length increases with an increase in barrier height (Table 3). In configurations from 1 to 3, which were used to simulate wind over urban terrains, the decrease in barrier height from *30* to *10 cm* reduced aerodynamics roughness

Table 1. Equations to calculate mean velocity, turbulence intensity, power-law index, and logarithmic law.

Mean velocity	Turbulence intensity	Power-law Index	Logarithmic Law
$\overline{U}_z = \int_0^T U(t)dt$	$I_z(z) = \dfrac{\sqrt{\overline{(u')^2}(z)}}{\overline{U}_z}$	$\dfrac{U_{z1}}{U_{z2}} = \left(\dfrac{z_1}{z_{ref}}\right)^{\alpha}$	$\dfrac{U(z)}{u^*} = \dfrac{1}{\kappa}\ln\left(\dfrac{z-d}{z_0}\right)$

Table 2. Equations to calculate autocorrelation coefficient, integral length scale, and integral length scale factor.

Autocorrelation coefficient	Integral length scale	Length scale factor
$Ru_x = \dfrac{\overline{[U(t)-\overline{U}(t)][U(t+\tau)-\overline{U}(t+\tau)]}}{\overline{U}^2}$	$Lu_x = \overline{U}\int_0^T Ru_x(\tau)d\tau$	$S = \dfrac{91.1(z)_m^{0.491}}{(Lu_x)_m^{1.403}(z_0)_m^{0.088}}$

Table 3. Various configurations of passive devices to reconstruct ABL.

No.	Configuration	u* (m/s)	α	z_0m	z_0p	S
1	F.R., B.H. = 30 cm, V.G. = 5, w = 0	1.451	0.28	6.38	3.94	617
2	F.R., B.H. = 20 cm, V.G. = 5, w = 0	1.553	0.27	4.68	3.34	713
3	F.R., B.H. = 10 cm, V.G. = 5, w = 0	1.548	0.25	3.84	2.91	759
4	F.R., B.H. = 30 cm, V.G. = 5, w = 10 cm	1.462	0.29	6.51	3.94	605
5	F.R., B.H. = 20 cm, V.G. = 5, w = 10 cm	1.563	0.28	4.91	3.34	681
6	F.R., B.H. = 10 cm, V.G. = 5, w = 10 cm	1.568	0.26	4.12	3.06	743
7	F.R., B.H. = 30 cm, V.G. = 5, w = 20 cm	1.474	0.31	6.91	3.9	565
8	F.R., B.H. = 20 cm, V.G. = 5, w = 20 cm	1.601	0.29	5.18	3.38	652
9	F.R., B.H. = 10 cm, V.G. = 5, w = 20 cm	1.611	0.28	4.72	3.36	712
10	H.R., B.H. = 30 cm, V.G. = 5, w = 0	1.406	0.27	4.12	2.82	685
11	H.R., B.H. = 20 cm, V.G. = 5, w = 0	1.421	0.25	2.37	1.96	829
12	H.R., B.H. = 10 cm, V.G. = 5, w = 0	1.431	0.23	2.08	1.80	868
13	H.R., B.H. = 30 cm, V.G. = 5, w = 10 cm	1.461	0.28	4.28	2.88	673
14	H.R., B.H. = 20 cm, V.G. = 5, w = 10 cm	1.428	0.25	2.46	1.95	792
15	H.R., B.H. = 10 cm, V.G. = 5, w = 10 cm	1.440	0.24	2.44	1.98	812
16	H.R., B.H. = 30 cm, V.G. = 5, w = 20 cm	1.400	0.29	4.41	2.94	666
17	H.R., B.H. = 20 cm, V.G. = 5, w = 20 cm	1.431	0.27	2.95	2.20	744
18	H.R., B.H. = 10 cm, V.G. = 5, w = 20 cm	1.429	0.26	2.56	2.00	782

F.R, Full roughness elements (72); H.R., half roughness elements (36); V.G., vortex generators, B.H., barrier height, *10 cm* one plank of *10 cm* with a gap of *10 cm* from the ground; *20 cm* two planks of *10 cm* each with a gap of *10 cm* between the two, *30 cm* three planks of *10 cm* each with a gap of *10 cm* between the two adjacent plank; w, slot width in the extended test section in the contraction zone.

length to 60% whereas configurations from 10 to 12 which presents rather suburban to rural terrains, the same decrease in barrier height reduced the aerodynamic roughness length to 64%. Similarly, due to the decrease in barrier height from *30* to *10 cm* (a) power-law exponent decreased, (b) shear velocity increased, and (c) model scale factor increased.

Effect of roughness bars on the wind characteristics

Only two sets (72 and 36) of the roughness bars were considered in this study. As shown in Table 3, more number of roughness elements on the floor assisted to (a) decrease the model scale factor, (b) increase power-law exponent, and (c) increase shear velocity.

With all these configurations, turbulence intensity was observed highest near the floor due to roughness bars, and barriers which reduced with the height.

Effect of slot width in the extended test section on the wind characteristics

Slot width in the extended test section in the contraction cone of the wind tunnel assisted to thicken the boundary
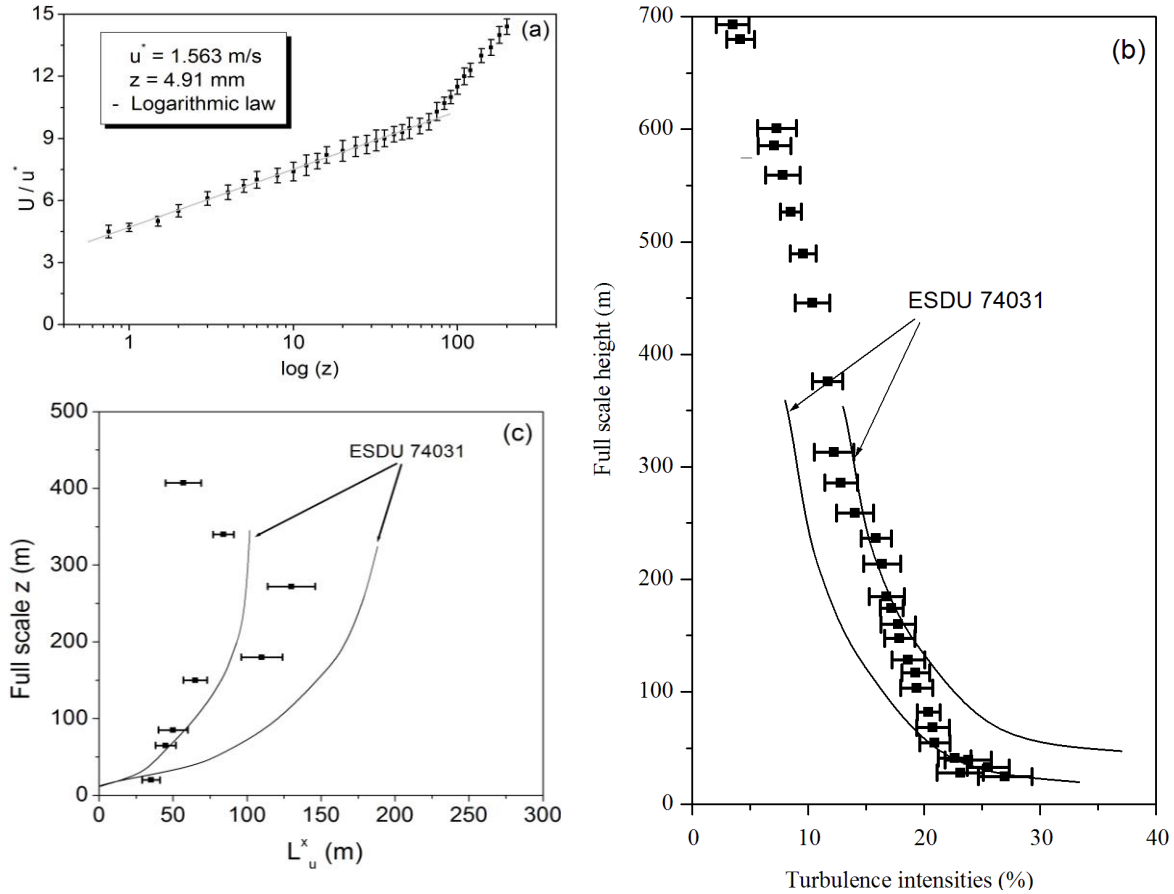
Figure 2. Wind properties for configuration 5. (a) Comparison of the mean velocity profile in 1:681 ABL simulations with the logarithmic law; (b) Longitudinal turbulence intensity profile, and (c) Longitudinal integral length scale profile. Vertical bars in (a) and horizontal bars in (b) and (c) give uncertainties due to finite number of measurements.

layer; however the effect of the variation in slot width on the wind characteristics is not very significant. The increase in the slot width, (a) decreased the model length scale factor slightly, (b) increased power-law exponent, and (c) increased shear velocity.

Conclusion

Wind characteristics over rural to urban terrains have been simulated in a boundary-layer wind tunnel with the assistance of passive roughness devices. Eighteen different configurations of the passive devices have been used and wind properties for each configuration have been calculated. The effect of each roughness device on the wind properties has been presented. It was found that the variation in the barrier height affect the wind properties significantly. Model length scale factor reduced to 60% by increasing the barrier height from *10 to 30 cm.* Likewise, more number of roughness elements on the floor also helped to decrease the model scale factor. The

slot width in the extended test section indeed helped to thicken the boundary layer however the effect of the variation in the slot width on the wind properties was not found to be very significant.

Nomenclature: U, Absolute velocity in x-direction; $\overline{U}$, mean velocity in x-direction; $\overline{U}_z$, mean velocity in x-direction at height z; u^*, shear velocity; U_{ref}, reference velocity; D, characteristic width; U_δ, free-stream velocity; R_e, Reynolds number; κ, von Kármán constant; w, slot

width; u', fluctuating velocity in x-direction; z_{ref}, reference height; x, distance in the direction of the flow; S, length scale factor; y, spanwise distance from test section centerplane; z, vertical distance from wind tunnel floor; z_0, aerodynamic surface roughness length; α, power law exponent; Lu_x, Longitudinal integral length scale; ν, air viscosity; Ru_x, longitudinal auto-correlation coefficient; δ, boundary layer thickness; m, model; P, prototype.

REFERENCES

Cook NJ (1978a). Determination of model-scale factor in wind tunnel simulations of the adiabatic boundary layer. J. Wind Eng. Ind. Aerod., 2(4): 311–321.

Cook NJ (1978b). Wind-tunnel simulation of adiabatic atmospheric boundary layer by roughness, barrier and mixing device method. J. Wind Eng. Ind. Aerod., 3(2-3): 157–176.

Counihan J (1969). An improved method of simulating an atmospheric boundary layer in a wind tunnel. Atmos. Environ., 3: 197–214.

Counihan J (1971). Wind tunnel determination of the roughness length as a function of the fetch and the roughness density of three-dimensional roughness elements. Atmos. Environ., 5: 637–642.

Counihan J (1973). Simulation of an adiabatic urban boundary layer in a wind tunnel. Atmos. Environ., 7: 673–689.

Counihan J (1975). Adiabatic atmospheric boundary layers: a review and analysis of data from the period 1880-1972. Atmos. Environ., 9: 871–905.

Cramer A, Varshney K, Gundrum T, Gerbeth G (2006). Experimental study on the sensitivity and accuracy of electric potential local flow measurements. Flow Meas. Instrum., 17: 1–11.

Davenport AG, Isyumov N (1967). The application of atmospheric boundary layer wind tunnel to prediction of wind loading, wind effects on buildings and structures. Univ. Toronto Press, Ottawa. pp. 210–230.

ESDU (1974-1975). Characteristics of atmospheric turbulence near the ground. Eng. Sci. Data Unit, London. pp. 74030-74031.

Farell C, Iyengar AKS (1999). Experiments on the wind tunnel simulation of atmospheric boundary layers. J. Wind Eng. Ind. Aerod., 79: 11–35.

Kozmar H (2010). Scale effects in wind tunnel modeling of an urban atmospheric boundary layer. Theor. Appl. Climatol., 100: 153–162.

Kozmar H (2011). Truncated vortex generators for part-depth wind-tunnel simulations of the atmospheric boundary layer flow. J. Wind Eng. Ind. Aerod., 99(2-3): 130–136.

Perry AE, Joubert PN (1963). Roughness boundary layers in adverse pressure gradients. J. Fluid Mech., 17: 193–221.

Reinhold TA, Tieleman HW, Maher FJ (1978). Simulation of the urban neutral boundary layer for the model study of wind loads on tall buildings. Depart. Eng. Sci. Mech. Virginia Polytechnic Instit. State Univ. Blacksburg. VPI-E-77-12.

Tieleman HW, Reinhold TA, Marshall RD (1978). Wind tunnel simulation of atmospheric surface layer for the study of wind loads on low-rise buildings. J. Wind Eng. Ind. Aerod., 3(1): 21–38.

Varshney K, Panigrahi PK (2005). Artificial neural network control of a heat exchanger in a closed flow air circuit. Appl. Soft Comput., 5: 441–465.

Varshney K, Rosa JE, Shapiro I (2011a). Method to diagnose window failures and measure U-factors on site. Int. J. Green Energy. In Press.

Varshney K, Poddar K (2011). Experiments on integral length scale control in atmospheric boundary layer wind tunnel. Theor. Appl. Climatol., 106: 127–137.

Varshney K, Poddar K (2012). Prediction of wind properties in urban environments using artificial neural network. Theor. Appl. Climatol., DOI: 10.1007/s00704-011-0506-9.

Varshney K, Shapiro I, Bronsnick Y, Holahan J (2011b). Air bypass in vertical stack water source heat pumps. HVAC&R Res., 17(5): 692-709.

Varshney K, Chang S, Wang ZJ (2012). The kinematics of falling maple seeds and the initial transition to a helical motion. Nonlinearity, 25(1): C1-C8.